Solvatochromic Shifts of Uracil and Cytosine Using a Combined Multireference Configuration Interaction/Molecular Dynamics Approach and the Fragment Molecular Orbital Method†

Kurt A. Kistler and Spiridoula Matsika*

Department of Chemistry, Temple University, Philadelphia, Pennsylvania 19122

Received: February 20, 2009; Revised Manuscript Received: May 14, 2009

A recently developed combined quantum mechanics/molecular mechanics (QM/MM) approach has been applied to the calculation of solvatochromic shifts of the excited states of the pyrimidine nucleobases uracil and cytosine in aqueous solution. In this procedure the quantum mechanical solute is described using a multireference configuration interaction method while molecular dynamics simulations are used to obtain the structure of the solvent around the solute. The fragment molecular orbital multiconfiguration self-consistent field (FMO-MCSCF) method of Fedorov and Kitaura is also used and compared with the QM/MM results. The two methods give similar results. The solvatochromic shifts in uracil are found to be +0.41 (+0.44) eV for the S_1 excited state and −0.05 (−0.19) eV for the S_2 state at the QM/MM (FMO-MCSCF) level. Solvatochromic shifts in cytosine are calculated to be +0.25 (+0.19), +0.56 (+0.62), and +0.83 (+0.83) eV for the S_1, S_2, and S_3 states, respectively, at the QM/MM (FMO-MCSCF) level.

1. Introduction

The excited states of nucleic acid bases have been studied extensively in the past because of their biological importance. The nucleobases are the primary chromophores in DNA and RNA absorbing UV radiation which may initiate photochemical reactions and subsequent photodamage.[1−3] For this reason the nature and dynamics of the excited states are particularly important, and much work has been done investigating them, experimentally and theoretically. Although most of the computational work has been done for the gas-phase nucleobases, one of the fundamental questions is how the solvent affects the excited states and their dynamical behavior.

Describing solvatochromic shifts with accurate ab initio methods is a challenging task involving two problems that are difficult to model even with modern quantum mechanical methods: the accurate description of solvent effects, and the accurate description of excited electronic states. As the size of the molecules increases the computational challenge increases even more rapidly making the study of solvated polyatomic molecules a far from trivial problem. There are various levels of sophistication for including solvent effects in the theoretical treatment of molecular systems, ranging from continuum models[4−6] to discrete representations.[7−9] Solvation effects on the nucleobases have been taken into account using explicit water molecules, continuum solvation models, or molecular dynamics (MD) simulations.[10−28]

Recently we developed a quantum mechanics/molecular mechanics (QM/MM) methodology that uses multireference configuration interaction (MRCI) to describe the quantum mechanical system.[29] The MRCI method is very suitable for the description of excited states, mixed character (multireference) states, and distorted geometries. The availability of analytic gradients for the MRCI wave functions makes it optimum for studies of excited states away from the Franck−Condon region and in nonadiabatic processes.[30−38] In order to utilize these advantages in solvated studies we combined high-level MRCI description for the solute and a detailed description of the solvent structure obtained from MD simulations using a classical force field. In this approach, the averaged solvent electrostatic potential (ASEP) in grid points enveloping the van der Waals surface of the molecule is calculated and represented by fitted partial charges. An effective Schrödinger equation, including this set of partial charges, is then solved providing ground- and excited-state wave functions and energies in the presence of the ASEP potential. This mean-field approach was originally developed by Aguilar and co-workers.[39−44] The method has been implemented in the COLUMBUS suite of programs[45−48] and tested previously in studies of the solvent effect on the $n_O\pi^*$ electronic transition in formaldehyde. Here it is used to study the pyrimidine bases uracil and cytosine (Figure 1) in aqueous phases. Our future goal is to extend our studies of excited-state relaxation mechanisms of cytosine and uracil in the gas phase to aqueous environments. In order to do so we are using and testing the QM/MM methodology for vertical absorptions, which have been extensively studied previously theoretically and experimentally.

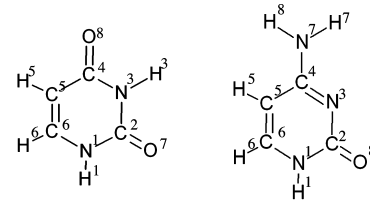

Figure 1. Uracil and cytosine labeling of the atoms.

The QM/MM approach utilized here can produce statistically converged results since it is able to use a very large number of configurations because of the averaging scheme used. The solvent molecules, however, are included in the QM calculation only as point charges fitted to reproduce the average potential. In order to test the accuracy of this approximation we also used

† Part of the "Russell M. Pitzer Festschrift".

* To whom correspondence should be addressed. E-mail: smatsika@temple.edu.

10.1021/jp901601u CCC: $40.75
Published on Web 06/08/2009

the fragment molecular orbital multiconfiguration self-consistent field (FMO-MCSCF) developed by Fedorov and Kitaura.[49] The FMO method provides an efficient way to treat large systems quantum mechanically, and it has been combined with a variety of quantum mechanical methods beyond HF, such as TDDFT, CIS, MCCSF, and CIS(D).[49−58] This method can treat both the solute and solvent quantum mechanically, and it can approach the accuracy of a full supersystem MCSCF calculation, with far less computational expense. The FMO-MCSCF method has been tested previously in various applications, but only one study has been published where the method is applied to calculate solvatochromic shifts.[49] In that example, the transition involved excitation of aqueous phenol from the ground-state singlet state to the first triplet state, thus involving different spin multiplicities. In this report we present, to the best of our knowledge, the first multistate excitation study of solvatochromism using FMO-MCSCF.

The methodological approaches used in this work, QM/MM and FMO, along with the computational details, are discussed in section 2, and results are presented and discussed in section 3.

2. Methodology

2.1. QM/MM. In a QM/MM approach the Hamiltonian for the whole system may be partitioned as

$$\hat{H} = \hat{H}_{QM} + \hat{H}_{MM} + \hat{H}_{QM/MM} \quad (1)$$

with terms that correspond to the quantum part, $\hat{H}_{QM}$, the classical part, $\hat{H}_{MM}$, and the interaction between them, $\hat{H}_{QM/MM}$. When studying solvent effects the separation in a quantum and classical part can be made naturally, with the quantum part involving only the solute molecule and the classical part including the solvent molecules. The quantum mechanical method chosen to describe the solute system here is a multireference approach which best describes excited states, specifically an MCSCF approach is used initially, followed by MRCI. The solvent is represented by classical force field interactions. The coupling between the two parts, $\hat{H}_{QM/MM}$, includes the electrostatic and van der Waals interactions between the quantum and classical particles.

In a usual QM/MM approach a QM calculation is performed for each configuration of a dynamical simulation. This approach requires thousands of QM calculations if statistical convergence is to be achieved. In order to avoid this bottleneck we have previously implemented a QM/MM method which uses an average approach introduced by Aguilar and co-workers.[39−44] The procedure begins by performing one quantum calculation for the solute molecule in the gas phase. The in vacuo solute geometry and partial charges are then used as input in the MD simulation. The quantum mechanical determination of the partial charges used here is based on the CHELPG (charges from electrostatic potentials using a grid-based method) algorithm.[59] Then a classical MD simulation is run to obtain the structure of the solvent around the solute. The electrostatic potential for all configurations is averaged to determine the ASEP, and this is fitted to a Coulomb potential produced by charges placed on a grid of points. The set of charges is produced by a least-squares fitting procedure which gives the best charges that can represent ASEP as an effective Coulomb potential. The final form introduced into the Hamiltonian is Coulomb interactions, with the charges now being fitted charges on a grid rather than atomic charges on the atoms. The electronic wave function of the solute in solution is obtained by solving the associated effective Schrödinger equation. More details of this approach can be found in our previous publication.[29]

TABLE 1: Force Field Parameters for Uracil and Cytosine

atom	σ (Å)	ϵ (kcal/mol)	fitted charge (e)
Uracil			
N^3	1.8240	0.1700	−0.7174
N^1	1.8240	0.1700	−0.5109
C^2	1.9080	0.0860	0.8919
C^6	1.9080	0.0860	0.1835
C^5	1.9080	0.0860	−0.5510
C^4	1.9080	0.0860	0.9362
O^8	1.6612	0.2100	−0.6271
O^7	1.6612	0.2100	−0.6374
H^3	0.6000	0.0157	0.3705
H^1	0.6000	0.0157	0.3335
H^6	0.6000	0.0157	0.1402
H^5	1.4590	0.0150	0.1880
Cytosine			
N^3	1.8240	0.1700	−0.8708
N^1	1.8240	0.1700	−0.6685
N^7	1.8240	0.1700	−0.7525
C^2	1.9080	0.0860	1.0817
C^6	1.9080	0.0860	0.3527
C^5	1.9080	0.0860	−0.6979
C^4	1.9080	0.0860	0.9246
O^8	1.6612	0.2100	−0.6773
H^1	0.6000	0.0157	0.3533
H^6	1.4090	0.0150	0.1039
H^5	1.4590	0.0150	0.2129
H^7	0.6000	0.0157	0.3335
H^8	0.6000	0.0157	0.3045

2.1.1. Molecular Dynamics Simulations. MD simulations using the MOLDY molecular dynamics package[60] were carried out in order to obtain the solvent structure around the solute molecules uracil and cytosine. A cubic box of edge 19.895 Å containing 257 (in uracil) or 260 (in cytosine) rigid water molecules and a rigid solute molecule at the temperature of 298 K and constant volume was used. Minimum image periodic boundary conditions[61] were applied, and the particle mesh Ewald sum[62−64] was used for charge interactions. The system was initially equilibrated for 2 ns, and then configurations were collected for another 2 ns. A time step of 0.5 fs was used throughout. Configurations were collected every 10 steps.

The rigid solute molecule has the gas-phase equilibrium geometry obtained at the quantum mechanical level of theory as described in section 2.1.2. This geometry was kept fixed in the MD simulation, since we focus on the vertical electronic transition. Table 1 lists the parameters used to describe the force field: the 6−12 type Lennard-Jones potential parameters σ, ϵ were taken from the Amber force field,[65] whereas the partial charges for each atomic center were obtained using CHELPG and a Hartree−Fock/cc-pVDZ wave function. These charges are not too different from AMBER charges, justifying the use of the remaining AMBER Lennard-Jones parameters. In general, the Lennard-Jones parameters should be optimized in combination with the charges in a particular force field, and problems may arise if one mixes parameters from different force fields. TIP3P parameters were used for water.[66]

2.1.2. Quantum Mechanical Calculations. The ground-state geometries of uracil and cytosine were optimized using MRCI and the cc-pVDZ basis set.[67] These geometries have been reported previously.[38,68] The excitation energy calculations were carried out at the MRCI level using the cc-pVDZ basis set and orbitals from a state-averaged MCSCF (SA-MCSCF) procedure. The details of the MCSCF and MRCI calculations were designed

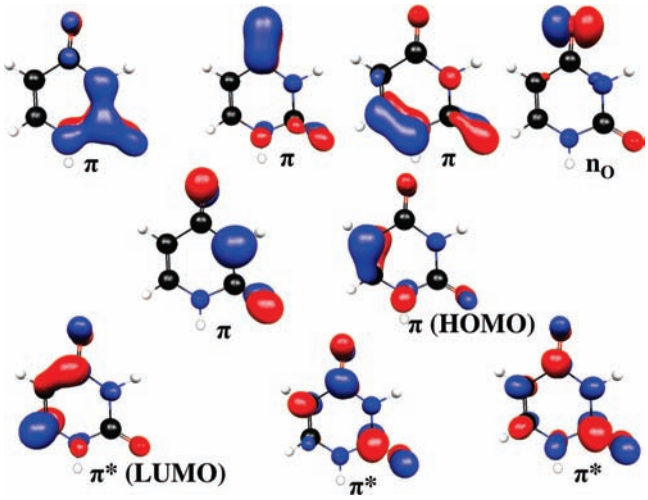

Figure 2. Molecular orbitals of uracil included in the active space.

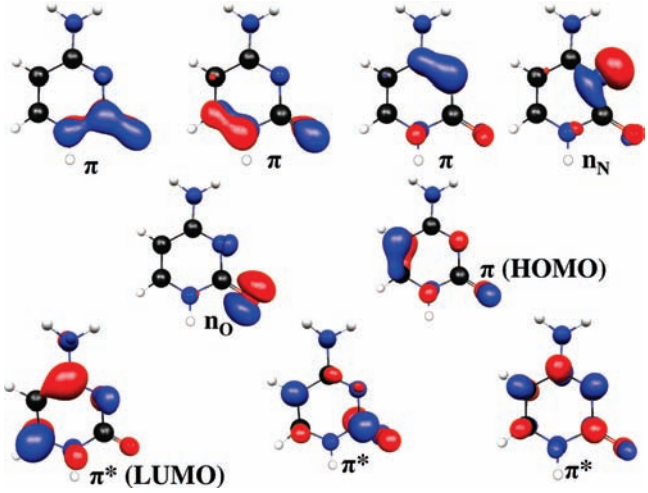

Figure 3. Molecular orbitals of cytosine included in the active space.

based on our previous experience and calculations on free uracil and cytosine.[38,68] In uracil the complete active space (CAS), for both the MCSCF and MRCI expansions, consists of 12 electrons in 9 molecular orbitals (MOs), denoted as (12,9), including all the π orbitals and one lone pair on oxygen, n_O. The active orbitals are shown in Figure 2. A three-state averaged MCSCF was used to obtain the orbitals. These choices were based on the fact that the first two excited states on uracil that are of interest to us in this work originate from excitation of a π or n_O orbital to a π^* orbital. The second n_O orbital does not affect the excitation energies a lot as we have seen in previous work.[38] In cytosine the active space in both MCSCF and MRCI is also a (12,9), which includes seven π orbitals and two lone pairs. The active orbitals are shown in Figure 3. The two lone pairs in cytosine are one on nitrogen and one on oxygen. Four states were used in the SA-MCSCF. The π electrons on the amino group do not affect the excitation energies significantly and have been excluded from the active space.

Two MRCI schemes were used, one denoted MRCI1, which allows only single excitations from the active space, and the second one denoted MRCI2, which allows single excitations from all orbitals, except the eight core 1s orbitals which are frozen, in addition to single and double excitations from the CAS. The resulting expansions for MRCI2 had ca. 112 million configuration state functions. The COLUMBUS[45−48] suite of programs was used for these calculations.

2.2. FMO-MCSCF. The effect of explicit water solvent molecules on the excitation energies of cytosine and uracil was studied with MCSCF using the multilayer formulation of the FMO-MCSCF method of Fedorov, Kitaura, and co-workers.[49−51] The QM/MM procedure outlined above does not take into account quantum interactions between the solvent and the solute or polarization between the solvent and the solute. In order to improve our description and estimate some of these effects, 60 configurations were taken from the MD simulations and used in FMO calculations. The configurations were chosen equally spaced in time during the simulation, taken every 25 ps. In some of the calculations only half of these configurations were used, again equally spaced in time (every 50 ps). Water molecules that were within a sphere of radius 7 Å from the atoms in the solute molecule were kept and included explicitly in the FMO calculations. This gave 37−48 water molecules with an average of 43 molecules surrounding the solute. The effect of the number of water molecules was tested, and it was found that the results do not change when more water molecules are included.

The FMO method has been described in detail previously.[49−58] Here we briefly present the important points, as they apply to the systems reported in this work. The system was divided into two layers, with layer 1 consisting of the waters, treated as separate individual molecules, or monomers, and layer 2 consisting of either a cytosine or a uracil, as the solute monomer. The geometry of the base was the same as in the QM/MM calculations, that of its gas-phase MRCI ground state, and its orientation was kept close to constant. The atomic orbital basis sets used were cc-pVDZ for the waters and either cc-pVDZ or cc-pVTZ for cytosine and uracil.[67] A restricted Hartree−Fock (RHF) calculation is performed for each monomer in the presence of the Coulomb field of all other monomers. The electrostatic potential from the rest of the monomers, $\boldsymbol{V}_x$, is calculated based on RHF densities

$$V^x_{\mu\nu} = \sum_{K\notin x}\left\{\sum_{A\in K}\langle\mu|-\frac{Z_A}{|\mathbf{r}-\mathbf{R}_A|}|\nu\rangle+\sum_{\rho\sigma\in K}D^K_{\rho\sigma}(\mu\nu|\rho\sigma)\right\} \quad (2)$$

and added to the Fock operator $\mathbf{F}$ to solve the FMO equations.

Here $x = I$ for monomers and $x = IJ$ for dimers (two monomers combined as one), Z_A and $\mathbf{R}_A$ are the nuclear charges and coordinates, respectively, for atom A, and μ, ν, ρ, and σ span the atomic orbitals. $\mathbf{D}^K$ is the density matrix of monomer K. An RHF calculation is carried out again for each monomer in the electrostatic potential generated by the other monomer densities, and this is repeated iteratively until the monomer densities for layer 1 are self-consistent. Dimers are then calculated using RHF, also in the potential of the rest of the monomer densities, first within layer 1, then as dimers formed between each water in layer 1 and the cytosine or uracil of layer 2. The inclusion of water−water and base−water dimers at the RHF level better describes hydrogen bonding quantum mechanically within each configuration and the commensurate effects on the MOs and densities of each monomer. Next, the MOs of the monomers of layer 1 are frozen, and the same RHF procedure is carried out on layer 2, which in this case contains only the base monomer. An SA-MCSCF calculation on the base monomer in layer 2 is then carried out for the first three or four singlet states, also in the potential generated by the RHF densities of the water molecules, using the same form for $\boldsymbol{V}_x$, as given above. The active space in the MCSCF is the same as in the gas phase and QM/MM calculations. FMO-MCSCF was carried out using GAMESS, version 24 MAR 2007 (R3).[69]

TABLE 2: Positions R_{max} and R_{min} (angstroms) and Amplitudes g_{max} and g_{min} of the Maxima and Minima of the First Peaks of Radial Distribution Functions

	R_{max}/R_{min}	g_{max}/g_{min}	R_{max}/R_{min} (AIMD)[a]	g_{max}/g_{min} (AIMD)[a]
Uracil				
H^1-O_w	1.95/2.55	0.98/0.42	1.80/2.50	1.06/0.37
H^3-O_w	1.95/2.55	1.15/0.31	1.80/2.40	1.00/0.17
O^8-H_w	1.85/2.45	1.17/0.26	1.80/2.50	1.15/0.24
O^7-H_w	1.85/2.45	1.17/0.26	1.80/2.30	1.36/0.25
Cytosine				
O^8-H_w	1.85/2.45	1.31/0.35		
N^3-H_w	1.95/2.65	0.65/0.20		
H^1-O_w	1.95/2.55	0.93/0.41		
H^7-O_w	2.15/2.55	0.63/0.51		
H^8-O_w	2.15/2.55	0.60/0.54		

[a] Previous AIMD results taken from ref 12.

In the multilayer form of FMO used here the exact dimer interactions are calculated at the RHF level while at the MCSCF level all pair interactions cancel out since they are the same for all states taken from the RHF of the ground state. At the MCSCF level the solute is interacting with the electron density of the solvent taken from the RHF level. Thus, any differential quantum effects between the electronic states are not included. Full polarization of the solvent is included in FMO unlike the QM/MM approach. The solvent density, however, is polarized through the ground state of the solute at the RHF level, and there is not any polarization due to the excited states.

2.3. Polarizable Continuum Model (PCM) Solvent. SA-MCSCF calculations were carried out for cytosine and uracil in water solvent described by a polarizable continuum model (PCM), as implemented in GAMESS.[70] A standard cavity was used where van der Waals radii were scaled by a scaling factor $f = 1.2$. The CASs were the same as described above, and the basis set was cc-pVDZ. Three states were averaged for uracil, whereas four states are averaged for cytosine, similarly to what was done in QM/MM and FMO.

3. Results and Discussion

3.1. Solvent Structure. Basic characteristics of the solvent structure of aqueous solutions of uracil and cytosine can be obtained from the MD simulations. The solvent structure of the solute in water is characterized by the radial distribution functions (RDFs). Table 2 lists the positions, R_{max}, R_{min}, and amplitudes, g_{max}, g_{min}, of the maxima and minima of the first peaks of the RDFs. The labeling of the atoms used in this table can be found in Figure 1.

In uracil the RDFs show that there are hydrogen bonds between the oxygen atoms on the carbonyls of uracil and hydrogen on water with lengths of 1.85 Å. The strength of the hydrogen bonds appears to be very similar for the two carbonyls. There are hydrogen bonds also between the hydrogen atoms on NH groups of uracil and oxygen on water. The hydrogen atoms on CH groups of uracil do not form clear hydrogen bonds, and the corresponding RDFs are broad without clear peaks at short distances. Our results on uracil are compared with previous ab initio "Car−Parrinello" molecular dynamics on aqueous uracil.[12] The RDFs peaks of that study are given in Table 2 as well. The "Car−Parrinello" results show the same type of hydrogen bonds as our results, although the R_{max} are somewhat shorter. Similarly to our results the RDFs corresponding to $CH-O_w$ were broad in that study as well. In that work the ratio g_{max}/g_{min} was used to compare the strength of H^1-O_w versus H^3-O_w hydrogen bonds. The ratio is higher for H^3-O_w indicating a stronger bond. This is also the case in our results. In general, comparison between our results and the more sophisticated "Car−Parrinello" results indicates that our MD dynamics describe solvation accurately enough to be used for the subsequent QM/MM studies.

In cytosine there are hydrogen bonds between the oxygen on carbonyl and hydrogen on water, O^8-H_w, N^3 and hydrogen on water, N^3-H_w, and also hydrogen bonds between the NH groups on cytosine and water oxygen. There are three such cases, H^1-O_w, H^7-O_w, and H^8-O_w. Clusters of cytosine with various numbers of water (between 3 and 13) display hydrogen bonds at the same sites.[71−73] The hydrogen-bond lengths from these cluster calculations were found to be O^8-H_w 1.9−2.1 Å, N^3-H_w 2.0 Å, H^1-O_w 2.0−2.1 Å, H^7-O_w and H^8-O_w 2.0−2.2 Å.

TABLE 3: Vertical Excitation Energy Shifts (eV) for Uracil in Aqueous Phase at Various Levels of Theory[a]

level of theory	S_1 ($n\pi^*$)	S_2 ($\pi\pi^*$)
MCSCF/cc-pVDZ	+0.40	−0.15
MRCI1/cc-pVDZ	+0.42	−0.11
MRCI2/cc-pVDZ	+0.41	−0.05
FMO-MCSCF/cc-pVDZ	+0.42 (0.44)	−0.16 (−0.19)
FMO-MCSCF/cc-pVTZ	+0.47	−0.18
MCSCF/PCM/cc-pVDZ	+0.24	−0.16
CCSD/SCRF[b]	+0.21	−0.07
CCSD/PMM[b]	+0.34	−0.12
TDDFT/PMM[b]	+0.38	−0.18
TD-PBE0/PMM[b]	+0.54	−0.10
TDDFT-PCM[c]	+0.29	−0.09
TDDFT-PCM+4H_2O[c]	+0.48	−0.10
INDO/CIS+200H_2O[d]	+0.50	−0.19
TDDFT/MC[d]	+0.80	−0.02
EOM-CCSDt/MM[e]	+0.44	+0.07

[a] In parentheses are FMO values using 60 configurations. Otherwise FMO results are obtained from 30 configurations. [b] Ref 13. [c] Ref 19. [d] Ref 24. [e] Ref 25.

3.2. QM/MM Results. ***3.2.1. Uracil.*** The excited states of uracil in vacuo have been studied theoretically previously with ab initio methods ranging from CIS to highly correlated complete active space with perturbation theory corrections (CASPT2) methods, MRCI, time-dependent density functional theory (TDDFT), and variants of coupled cluster.[10,13,14,16,22,25,38,74−82] The first excited state, S_1, is a dark $n_O\pi^*$ state, whereas the second excited state, S_2, is a bright $\pi\pi^*$ state. The orbitals involved in the excitations are shown in Figure 2. S_1 is primarily an excitation from the n_O to the π^* (LUMO) orbital, whereas S_2 is primarily an excitation from π (HOMO) to π^* (LUMO). The excitation energies for these states vary considerably depending on the method used, especially for the $\pi\pi^*$ state. A recent benchmark study using high-level completely renormalized equation-of-motion coupled cluster method with single, double, and approximate triple excitations (CR-EOM-CCSD(T)) and MRCI methods, in combination with large basis sets, provides the best estimates for the excitation energies to be 5.0 ± 0.1 and 5.3 ± 0.1 eV for the S_1 and S_2 states, respectively.[25] The MRCI2 expansion used here predicts these excitation energies 5.20 and 5.90 eV. As we will see below, although the excitation energies are very difficult to calculate accurately, the solvatochromic shifts do not depend much on the level of correlation.

In Table 3, the calculated vertical excitation energy shifts for aqueous uracil are given using QM/MM and the MCSCF, MRCI1, and MRCI2 quantum mechanical levels. All methods predict a blue-shift for the first $n\pi^*$ state and a red-shift for the

TABLE 4: Vertical Excitation Energy Shifts (in eV) of Cytosine in Aqueous Phase at Various Levels of Theory[a]

level of theory	S_1 ($\pi\pi^*$)	S_2 ($n\pi^*$)	S_3 ($n\pi^*$)
MCSCF/cc-pVDZ	+0.20	+0.56	+0.72
MRCI1/cc-pVDZ	+0.17	+0.56	+0.76
MRCI2/cc-pVDZ	+0.25	+0.56	+0.83
FMO-MCSCF/cc-pVDZ	+0.19 (0.19)	+0.63 (0.62)	+0.82 (0.83)
FMO-MCSCF/cc-pVTZ	+0.18	+0.65	+0.85
MCSCF/PCM/cc-pVDZ	+0.03	+0.23	+0.28
scaled CIS+3H_2O[b]	+0.10	+0.35	+0.31
TD-DFT+3H_2O[b]	+0.18	+0.45	+0.43
EOM-CCSD/MM[c,d]	+0.25	+0.57	
CR-EOM-CCSD(T)/MM[c,d]	+0.25	+0.54	
CASSCF/CPCM[e]	+0.2	+0.6	+0.8

[a] In parentheses are FMO values using 60 configurations. Otherwise FMO results are obtained from 30 configurations. [b] Ref 15. [c] Cytosine in native DNA environment. [d] Ref 26. [e] Ref 27.

first $\pi\pi^*$ state, as expected based on the dipole moments of these states. Each state is stabilized in the presence of the electrostatic interactions with the solvent. If the dipole moment of the excited state is smaller than that of the ground state the excited state is stabilized less than the ground state resulting in an increased excitation energy, and a blue-shift is observed in absorption spectra. If, on the other hand, the excited state has a larger dipole moment than the ground state the opposite effect is observed. In uracil the S_0, S_1, and S_2 states have dipole moments with magnitudes 4.17, 1.68, and 5.53 D, respectively (calculated at the MRCI2 level). The blue-shift for the first $n\pi^*$ state is +0.41 eV, and the red-shift for the first $\pi\pi^*$ state is −0.05 eV at the MRCI2 level. The shift of the S_1 state does not change much with the addition of correlation (ranging between 0.40 and 0.42 eV), whereas S_2 is more sensitive, with the magnitude of the red-shift decreasing by 0.1 eV with inclusion of correlation (0.05−0.15 eV).

3.2.2. Cytosine. The excited states of cytosine have also been studied theoretically previously with a variety of ab initio methods.[68,78,81−91] The S_1 state is a $\pi\pi^*$ excitation, whereas S_2 and S_3 are dark states with excitations from the lone pairs on nitrogen and oxygen. The orbitals involved in the excitations are shown in Figure 3, where the S_1 state involves primarily the π (HOMO) and π^* (LUMO) orbitals, whereas S_2 and S_3 involved the n_O, n_N, and π^* (LUMO). The excitation energies and even the ordering of the states are very sensitive to the method chosen. High-level CR-EOM-CCSD(T) calculations predict the S_1 and S_2 states to have vertical excitation energies 4.76 and 5.24 eV.[26] The present MRCI2 calculations give 5.14, 5.29, and 5.93 eV for the S_1, S_2, and S_3 states, respectively.

In Table 4, the calculated vertical excitation energy shifts for aqueous cytosine calculated using our QM/MM approach are shown. As discussed earlier the magnitude of the solvatochromic shift for each state depends on the dipole moment of that state, where the state that has the largest difference of dipole moment with the ground state will have the largest shift. The dipole moments of the S_0, S_1, S_2, and S_3 states are calculated to be 5.90, 4.33, 2.32, and 1.72 D, respectively, as we reported previously.[68] Thus, all excited states are blue-shifted in aqueous solution, and the magnitude of the shifts increases in the order $S_1 < S_2 < S_3$. The S_1 state has the smaller shift, 0.25 eV, whereas the shift is much higher for the $n\pi^*$ states S_2 and S_3, 0.56 and 0.83 eV, respectively, at the MRCI2 level. The shift of the S_1 state varies by 0.08 eV depending on how much correlation is included at the QM level, and the shift of S_3 varies by 0.11 eV. The S_2 shift on the other hand is insensitive to correlation.

The QM/MM approach is advantageous since it can produce statistically converged results by using a very large number of configurations in the averaging scheme used. The solvent molecules, however, are included in the QM calculation only as point charges fitted to reproduce the average potential. So there are many effects that are missing in the treatment and can produce potential errors. The solvent is not polarizable since we did not use polarizable force fields, and quantum interactions between the solvent and the solute are not included since we are only treating the solvent with point charges. The point charges can also produce overpolarization of the quantum mechanical solute as has discussed in the literature.[92,93] Various methods exist which can include some of the missing effects. In order to check how much these missing effects change our results we then discuss shifts produced using the FMO method and compare them to the QM/MM ones.

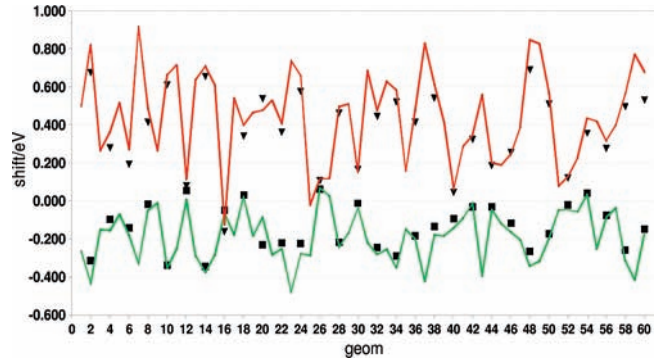

Figure 4. Solvatochromic shifts in uracil calculated using the FMO method and using the point charges only on water for selected configurations. Solid colored lines connect FMO-MCSCF points: red is S_1 shift, green is S_2 shift. Unconnected black symbols are QM/MM points: triangles are S_1 shifts, squares are S_2 shifts.

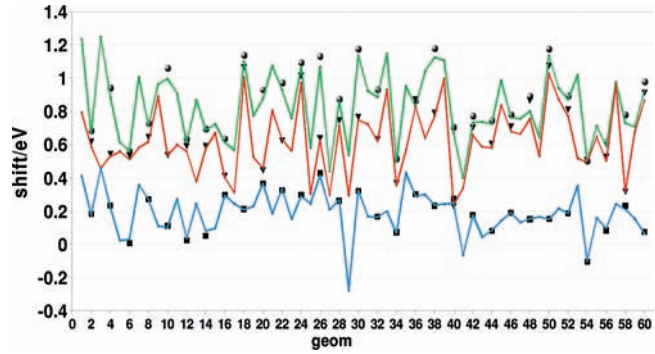

Figure 5. Solvatochromic shifts in cytosine calculated using the FMO method for selected configurations. Solid colored lines connect cc-pVDZ points: blue is S_1 shift, red is S_2 shift, green is S_3 shift. Large unconnected symbols are cc-pVTZ points: squares are S_1 shifts, triangles are S_2 shifts, and spheres are S_3 shifts.

3.3. FMO-MCSCF Results. The FMO method has also been used to calculate the solvatochromic shifts in uracil and cytosine. This method is currently implemented at the MCSCF level, so comparisons between the QM/MM and FMO methods will only be done at this level using the cc-pVDZ basis set for consistency. The solvatochromic shifts for each of the 60 snapshots in uracil and cytosine using the FMO-MCSCF method are shown in Figures 4 and 5, respectively. The averages of these shifts are given in Tables 3 and 4. The average solvatochromic shift in uracil using FMO-MCSCF was calculated to be +0.44 eV for the S_1 $n_O\pi^*$ state and −0.19 eV for the S_2 $\pi\pi^*$ state. Using QM/MM at the MCSCF level, the corresponding shifts are +0.40 and −0.15 eV, differing from FMO by 0.04 eV in both cases. Similarly the solvatochromic shifts of the first three excited singlet states in cytosine were computed using the FMO-

MCSCF method, using cc-pVDZ. All three excited states showed blue-shifting compared to gas phase. These shifts were calculated to be 0.19, 0.62, and 0.83 eV for the S_1, S_2, and S_3 states, respectively. The corresponding shifts at the QM/MM level using MCSCF are 0.20, 0.56, and 0.72 eV. Here QM/MM, when compared to FMO, overestimates the S_1 shift by 0.01 eV and underestimates the S_2 and S_3 shifts by 0.06 and 0.11 eV, respectively. The differences between FMO and QM/MM are small again although they are somewhat larger for the S_2 and S_3 states, possibly reflecting a better description of hydrogen bonds.

The FMO method as used here included only the base in layer 2, and thus no dimer calculations have been done at the MCSCF level. Previous work has shown that the error of this approximation on excitation energies is about 0.01 eV, and it was shown that the static correlation included at the MCSCF level has a local character. Thus, it was decided that it is sufficient to do MCSCF on the monomer only.[49] We also performed our own tests to check the importance of doing MCSCF calculations for dimers. We used four different isomers of uracil with one water molecule previously reported as the most stable minima.[94] For each of these structures we compared full MCSCF results for the dimers with results from an FMO procedure similar to the one used here where the MCSCF is done only for one monomer, uracil. The total ground-state energy between the two methods differs by 0.001−0.002 hartree. The excitation energies differ by 0.001−0.043 eV with an average of 0.02 eV. These results agree with the previous conclusion that omitting a full dimer MCSCF calculation introduces only small errors.

The FMO values are very close to the values predicted with the QM/MM procedure, but there are many factors that are different between the two calculations, and the agreement could be partly due to combination of competing effects. In order to check individual effects we chose half of the initial 60 configurations for additional comparisons. The average of these 30 configurations are also reported in Tables 3 and 4. The average change when reducing the number of configurations to half is 0.014 eV. In order to compare more directly the classical and quantum effects, the 30 configurations of uracil in water were used in a calculation where the waters were included into the calculation as point charges (using TIP3P values) and the shifts were calculated at the MCSCF level. These calculations gave an average shift of 0.37 eV for the S_1 state and −0.14 eV for S_2 compared to 0.42 and −0.16 eV, respectively, at the FMO level. So classical charges underestimate the blue-shift of S_1 by 0.05 eV and the red-shift of S_2 by 0.02 eV compared to the FMO results. The results for each configuration are shown in Figure 4 in comparison with the FMO results. If the deviations of the individual configurations are monitored explicitly the maximum underestimates are 0.05 eV for S_1 and 0.03 eV for S_2. Overall we may assume that the estimated error of using point charges and purely electrostatic interactions without considering the polarization of the solvent is on the order of 0.05 eV. Figure 4 also shows how the different individual configurations can have a wide range of solvatochromic shifts depending on the arrangement of water molecules around the solute and the number of hydrogen bonds in each case.

The effect of the basis set was also investigated using the FMO method. Within the FMO-MCSCF method it is possible to use different basis sets for the atoms in different layers, so we only changed the basis set to cc-pVTZ for the solute and used cc-pVDZ for water, since the cost does not increase dramatically if only the solute uses a larger basis set. Attempts to use basis sets with diffuse functions were unsuccessful for technical reasons, so we limit our comparisons to the above two basis sets. The same 30 configurations were recalculated using FMO-MCSCF. In uracil the shifts using the cc-pVTZ basis set are 0.47 and −0.18 eV compared to 0.42 and −0.16 eV using the cc-pVDZ basis set. The increased basis set changes the shift by 0.05 and 0.02 eV for the two states. In cytosine the shifts when using cc-pVTZ were calculated to be 0.18, 0.65, and 0.85 eV for the S_1, S_2, and S_3 states, respectively. These differ from the cc-pVDZ results by 0.01, 0.02, 0.03 eV for the S_1, S_2, and S_3 states, respectively. Thus, the effect of the larger basis set is small. For both molecules the $n\pi^*$ states are somewhat more sensitive to the basis set.

Since the MOs for the base monomer distort from polarization due to the surrounding waters, but remain a separate MO set in these FMO-MCSCF calculations, it is possible to do a gas-phase complete active space configuration interaction (CAS-CI) calculation using these polarized MOs to analyze the shifting effect of orbital polarization on the excited states, without the solvent electrostatic interaction present. For cytosine using cc-pVTZ the average shifts, all blue, were 0.01, 0.05, and 0.05 eV for the S_1, S_2, and S_3 states, respectively. The remainder of the total shifts given above are from electrostatics. However, the standard deviations for these polarization shifts were each about 0.05 eV, making generalizations about these shifts difficult, other than the fact that they are small compared to the electrostatic interaction, and on average the $n\pi^*$ states are blue-shifted more than the $\pi\pi^*$ state.

3.4. PCM Results. The solvatochromic shifts in uracil (cc-pVDZ) when PCM water was applied to the MCSCF calculation were 0.24 eV for the S_1 state and −0.16 eV for the S_2 state. Thus, although PCM does well in predicting the shift for the $\pi\pi^*$ state, the shift for the $n_O\pi^*$ state is underestimated significantly. In cytosine (cc-pVDZ) the shifts using PCM water were 0.03 eV for S_1, 0.23 eV for S_2, and 0.28 eV for S_3, and all three of these shifts are quite underestimated compared to QM/MM or FMO-MCSCF. These results underscore the importance of an explicit solvent model in determining aqueous solvatochromic shifts, both classically, as in the case of QM/MM, and especially quantum mechanically, as in the case of FMO-MCSCF. Previous work using continuum models also showed the same trends of underestimating the solvatochromic shifts for these molecules, as can be seen in Tables 3 and 4.

Solvatochromic shifts predicted with dielectric continuum solvation models are often underestimated in aqueous solutions where hydrogen bonds are involved, as has been seen before.[95,96] Supermolecular calculations where one or more water molecules are treated explicitly and then are solvated with the dielectric continuum can improve the shifts, and this approach has been used by others for uracil and cytosine.[19,23,27] It has also been observed that the PCM shifts are very sensitive to the radii, and specifically, changing the scaling factor from $f = 1.2$ to a smaller value will increase the shifts.[96] We tested this in our calculations as well and found that decreasing f increases the shifts in cytosine and brings them closer to the QM/MM and FMO results. Changing the scaling factor seems arbitrary, however, and PCM is used here solely for comparisons, so we only report the standard results.

3.5. Comparison with Previous Work. Solvation effects on uracil and its excited states have been studied theoretically in the past using both explicit and implicit models.[13,16,18−25,28] Continuum solvation models in general underestimate the shifts. Some results are listed in Table 3. In a TDDFT-PCM study the shifts increased substantially when four explicit water molecules

were added in this calculation, demonstrating the importance of the explicit interactions. This is in agreement with the present calculations in which the PCM model predicted a shift of 0.24 eV, much lower than the values of QM/MM and FMO methods. Zazza et al.[13] used the perturbed matrix method (PMM) in combination with TDDFT and CCSD to calculate the solvatochromic shifts. They obtained a shift for the S_1 state ranging between (+0.34) and (+0.54) eV and for the S_2 between (−0.10) and (−0.18) eV, depending on the level of quantum mechanical method for the solute. Monte Carlo simulations have also been used to generate solvation configurations that were subsequently used in QM calculations.[24] These results using 200 water molecules and the semiempirical INDO method suggest solvatochromic shifts of 0.50 and −0.19 eV for S_1 and S_2, respectively. MD simulations were used in connection with high-level ab initio EOM-CCSDt methods (active space EOMCCSDt approximations include the effect of triples in an iterative way) for the solvent to give a +0.44 eV blue-shift for S_1 and a small blue-shift for the S_2 state. Our results for S_1 are within 0.4−0.5 eV, which is the range predicted by other high-level methods. Our S_2 shifts are −0.05 to −0.2 eV, again within the values predicted by other methods.

Experimental spectra of uracil exist in the gas phase and aqueous solution. The assignment of states, however, is difficult, particularly for the dark state. Absorption spectra of aqueous uracil show a bright band at 4.8 eV, which is the $\pi\pi^*$ state, and the solvatochromic shift is estimated to be ca. 0.2 eV.[97−99] The $n\pi^*$ state is much more difficult to observe experimentally, although some work suggests that the blue-shift is ca. 0.5 eV.

Solvatochromic shifts for cytosine have also been calculated with a variety of methods. Shukla and Leszczynski[15] studied clusters of cytosine and three water molecules with CIS and TDDFT methods to obtain solvatochromic shifts. More sophisticated calculations have appeared recently. Blancafort and Migani[27] used a CASSCF approach combined with the conductor version of the polarizable continuous (CPCM) model for cytosine plus an explicit water hydrogen-bonded to it to calculate the shifts, which were subsequently added to CASPT2 excitation energies. They obtained values of +0.2, +0.6, +0.8 eV for the shifts of S_1, S_2, and S_3 states, respectively. Valiev and Kowalski used a CR-EOM-CCSD(T) and a classical MD approach to calculate the solvatochromic shifts of the excited states of cytosine in the native DNA environment.[26] The CR-EOM-CCSD(T)/MM method predicts S_1 to be blue-shifted by 0.25 eV, and S_2 by 0.54 eV.[26] Our QM/MM and FMO results are in reasonable agreement with these results.

The experimental results reported in the spectra of cytosine are very discrepant. Clark et al.[100] reported 4.28 eV for the S_0-S_1 excitation energy in gas phase and 4.64 eV for aqueous phase, which gives a blue-shift of +0.36 eV. More recently Abouaf et al.[101] reported 4.65 ± 0.1 eV for the S_0-S_1 excitation energy in gas phase, which implies a much smaller solvent shift.[102]

4. Conclusions

Solvatochromic shifts for the excited states of uracil and cytosine were calculated using two methods, a recently developed QM/MM and the FMO-MCSCF method. Both methods used configurations created by the same MD simulations. Using the same solvent structure created by this simulation these methods gave similar results. The MRCI2/MM (FMO-MCSCF) results for the solvatochromic shifts are, in uracil, +0.41 (+0.44) eV for the S_1 excited state ($n\pi^*$) and −0.05 (−0.19) eV for the S_2 state ($\pi\pi^*$) and, in cytosine, +0.25 (+0.19), +0.56 (+0.62), and +0.83 (+0.83) eV for the S_1, S_2, and S_3 states, respectively. These results agree well with other previously reported high-level calculations. It can be concluded that our QM/MM approach can reasonably predict the solvatochromic shifts in these molecules, and the error of not including explicit quantum mechanically described solvent molecules is less than 0.1 eV. The FMO-MCSCF method gives results that agree well with other more correlated methods, showing great potential as an alternative method to calculate solvated molecules. Continuum models, on the other hand, are not adequate to describe the interactions and underestimate significantly the magnitude of the solvatochromic shifts. Correlation effects are predicted to be 0.01−0.1 eV, and the effect of increasing the basis set from a cc-pVDZ to a cc-pVTZ is 0.01−0.07 eV. Thus, the solvatochromic shifts are shown to be much less sensitive to the quantum mechanical level of theory used compared to actual excitation energies.

Acknowledgment. This work was supported by the National Science Foundation under Grant No. CHE-0449853 and Temple University. K.A.K. is partially supported by a Case Fellowship. We thank Costantino Zazza for lending us his MD simulation data for testing and comparisons and Dmitri Fedorov for helpful discussions about FMO.

References and Notes

(1) Crespo-Hernandez, C. E.; Cohen, B.; Hare, P. M.; Kohler, B. *Chem. Rev.* **2004**, *104*, 1977.
(2) Cadet, J.; Vigny, P. In *Bioorganic Photochemistry*; Morrison, H., Ed.; Wiley: New York, 1990; Vol. 1; p 1.
(3) Ruzsicska, B. P.; Lemaire, D. G. E. In *CRC Handbook of Organic Photochemistry and Photobiology*; Horspool, W. M., Song, P. S., Eds.; CRC Press: Boca Raton, FL, 1995; p 1289.
(4) Tomasi, J.; Persico, M. *Chem. Rev.* **1994**, *94*, 2027.
(5) Cramer, C. J.; Truhlar, C. J. In *Reviews in Computational Chemistry*; Lipkowitz, K. B., Boyd, D. B., Eds.; Wiley-VCH: New York, 1995; Vol. 6, p 1.
(6) Tomasi, J.; Mennucci, B.; Cammi, R. *Chem. Rev.* **2005**, *105*, 2999.
(7) Gao, J. In *Reviews in Computational Chemistry*; Lipkowitz, K. B., Boyd, D. B., Eds.; Wiley-VCH: New York, 1996; Vol. 7, p 119.
(8) Gao, J. *Acc. Chem. Res.* **1996**, *19*, 298.
(9) Orozco, M.; Luque, F. J. *Chem. Rev.* **2000**, *100*, 4187.
(10) Broo, A.; Holmén, A. *J. Phys. Chem. A* **1997**, *101*, 3589.
(11) Mennucci, B.; Toniolo, A.; Tomasi, J. *J. Phys. Chem. A* **2001**, *105*, 4749.
(12) Gaigeot, M. P.; Sprik, M. *J. Phys. Chem. B* **2004**, *108*, 7458.
(13) Zazza, C.; Amadei, A.; Sanna, N.; Grandi, A.; Chillemi, G.; Nola, A. D.; D'Abramo, M.; Aschi, M. *Phys. Chem. Chem. Phys.* **2006**, *8*, 1385–1393.
(14) Shukla, M. K.; Mishra, P. C. *Chem. Phys.* **1999**, *240*, 319.
(15) Shukla, M. K.; Leszczynski, J. *J. Phys. Chem. A* **2002**, *106*, 11338.
(16) Shukla, M. K.; Leszczynski, J. *J. Phys. Chem. A* **2002**, *106*, 8642.
(17) Shukla, M. K.; Leszczynski, J. *J. Phys. Chem. B* **2005**, *109*, 17333–17339.
(18) Gustavsson, T.; Banyasz, A.; Lazzarotto, E.; Markovitsi, D.; Scalmani, G.; Frisch, M. J.; Baron, V.; Improta, R. *J. Am. Chem. Soc.* **2006**, *128*, 607–619.
(19) Improta, R.; Barone, V. *J. Am. Chem. Soc.* **2004**, *126*, 14320.
(20) Gustavsson, T.; Sarkar, N.; Lazzarotto, E.; Markovitsi, D.; Improta, R. *Chem. Phys. Lett.* **2006**, *429*, 551–557.
(21) Zhang, R. B.; Zeegers-Huyskens, T.; Ceulemans, A.; Nguyen, M. T. *Chem. Phys.* **2005**, *316*, 35.
(22) Marian, C. M.; Schneidaer, F.; Kleinschmidt, M.; Tatchen, J. *Eur. Phys. J. D* **2002**, *20*, 357.
(23) Santoro, F.; Barone, V.; Gustavsson, T.; Improta, R. *J. Am. Chem. Soc.* **2006**, *128*, 16312–16322.
(24) Ludwig, V.; Coutinho, K.; Canuto, S. *Phys. Chem. Chem. Phys.* **2007**, *9*, 4907–4912.
(25) Epifanovsky, E.; Kowalski, K.; Fan, P. D.; Valiev, M.; Matsika, S.; Krylov, A. I. *J. Phys. Chem. A* **2008**, *112*, 9983–9992.
(26) Valiev, M.; Kowalski, K. *J. Chem. Phys.* **2006**, *125*, 211101.
(27) Blancafort, L.; Migani, A. *J. Photochem. Photobiol., A* **2007**, *190*, 283–289.
(28) Busker, M.; Nispel, M.; Häber, T.; Kleinermanns, K.; Etinski, M.; Fleig, T. *Chem. Phys. Chem.* **2008**, *9*, 1570–1577.
(29) Xu, Z.; Matsika, S. *J. Phys. Chem. A* **2006**, *110*, 12035–12043.
(30) Jørgensen, P.; Simons, J. *J. Chem. Phys.* **1983**, *79*, 334.

(31) Page, M.; Saxe, P.; Adams, G. F.; Lengsfield, B. H. *J. Chem. Phys.* **1984**, *81*, 434.
(32) Helgaker, T.; Almlöf, J. *Int. J. Quantum Chem.* **1984**, *26*, 275.
(33) Shepard, R. In *Modern Electronic Structure Theory Part I*; Yarkony, D. R., Ed.; World Scientific: Singapore, 1995; p 345.
(34) Lischka, H.; Dallos, M.; Shepard, R. *Mol. Phys.* **2002**, *100*, 1647.
(35) Lischka, H.; Dallos, M.; Szalay, P. G.; Yarkony, D. R.; Shepard, R. *J. Chem. Phys.* **2004**, *120*, 7322.
(36) Dallos, M.; Lischka, H.; Shepard, R.; Yarkony, D. R.; Szalay, P. G. *J. Chem. Phys.* **2004**, *120*, 7330.
(37) Matsika, S.; Yarkony, D. R. *J. Chem. Phys.* **2002**, *117*, 6907.
(38) Matsika, S. *J. Phys. Chem. A* **2004**, *108*, 7584.
(39) Sánchez, M. L.; Aguilar, M. A.; Olivares del Valle, F. J. *J. Comput. Chem.* **1997**, *18*, 313.
(40) Sánchez, M. L.; Martín, M. E.; Aguilar, M. A.; Olivares del Valle, F. J. *Chem. Phys. Lett.* **1999**, *310*, 195–200.
(41) Martín, M. E.; Sanchez, M. L.; Olivares Del Valle, F. J.; Aguilar, M. A. *J. Chem. Phys.* **2000**, *113*, 6308.
(42) Sánchez, M. L.; Aguilar, M. A.; Olivares del Valle, F. J. *J. Mol. Struct. (THEOCHEM)* **1997**, *426*, 181.
(43) Fdez. Galván, I.; Sánchez, M. L.; Martín, M. E.; Olivares del Valle, F.; Aguilar, M. *J. Chem. Phys.* **2000**, *21*, 705.
(44) Sánchez, M. L.; Martín, M. E.; Aguilar, M.; Olivares del Valle, F. *J. Comput. Chem.* **2000**, *21*, 705.
(45) Lischka, H.; Shepard, R.; Brown, F. B.; Shavitt, I. *Int. J. Quantum Chem., Symp.* **1981**, *15*, 91–100.
(46) Shepard, R.; Shavitt, I.; Pitzer, R. M.; Comeau, D. C.; Pepper, M.; Lischka, H.; Szalay, P. G.; Ahlrichs, R.; Brown, F. B.; Zhao, J. *Int. J. Quantum Chem., Quantum Chem. Symp.* **1988**, *22*, 149.
(47) Lischka, H.; Shepard, R.; Pitzer, R. M.; Shavitt, I.; Dallos, M.; Müller, Th.; Szalay, P. G.; Seth, M.; Kedziora, G. S.; Yabushita, S.; Zhang, Z. *Phys. Chem. Chem. Phys.* **2001**, *3*, 664.
(48) Lischka, H.; Shepard, R.; Shavitt, I.; Pitzer, R. M.; Dallos, M.; Müller, T.; Szalay, P. G.; Brown, F. B.; Ahlrichs, R.; Böhm, H. J.; Chang, A.; Comeau, D. C.; Gdanitz, R.; Dachsel, H.; Ehrhardt, C.; Ernzerhof, M.; Hchtl, P.; Irle, S.; Kedziora, G.; Kovar, T.; Parasuk, V.; Pepper, M. J. M.; Scharf, P.; Schiffer, H.; Schindler, M.; Schüler, M.; Seth, M.; Stahlberg, E. A.; Zhao, J.-G.; Yabushita, S.; Zhang, Z.; Barbatti, M.; Matsika, S.; Schuurmann, M.; Yarkony, D. R.; Brozell, S. R.; Beck, E. V.; Blaudeau, J.-P. COLUMBUS, an Ab Initio Electronic Structure Program, release 5.9.1, 2006.
(49) Fedorov, D. G.; Kitaura, K. *J. Chem. Phys.* **2005**, *122*, 054108.
(50) Kitaura, K.; Ikeo, E.; Asada, T.; Nakano, T.; Uebayasi, M. *Chem. Phys. Lett.* **1999**, *313*, 701–706.
(51) Fedorov, D. G.; Ishida, T.; Kitaura, K. *J. Phys. Chem. A* **2005**, *109*, 2638–2646.
(52) Chiba, M.; Fedorov, D. G.; Kitaura, K. *Chem. Phys. Lett.* **2007**, *444*, 346–350.
(53) Chiba, M.; Fedorov, D. G.; Kitaura, K. *J. Chem. Phys.* **2007**, *127*, 104108.
(54) Chiba, M.; Fedorov, D. G.; Kitaura, K. *J. Comput. Chem.* **2008**, *29*, 2667–2676.
(55) Fedorov, D. G.; Kitaura, K. *J. Phys. Chem. A* **2007**, *111*, 6904.
(56) Mochizuki, Y.; Koikegami, S.; Amari, S.; Segawa, K.; Kitaura, K.; Nakano, T. *Chem. Phys. Lett.* **2005**, *406*, 283–288.
(57) Mochizuki, Y.; Komeiji, Y.; Ishikawa, T.; Nakano, T.; Yamataka, H. *Chem. Phys. Lett.* **2007**, *437*, 66–72.
(58) Mochizuki, Y.; Tanaka, K.; Yamashita, K.; Ishikawa, T.; Nakano, T.; Amari, S.; Segawa, K.; Murase, T.; Tokiwa, H.; Sakurai, M. *Theor. Chem. Acc.* **2007**, *117*, 541.
(59) Chirlian, L. E.; Francl, M. M. *J. Comput. Chem.* **1987**, *8*, 894.
(60) Refson, K. *Comput. Phys. Commun.* **2000**, *126*, 309–328.
(61) Leach, A. R. *Molecular Modelling Principles and Applications*; Prentice Hall: Dorchester, MA, 2001.
(62) Hockney, R. W.; Eastwood, J. W. *Computer Simulation Using Particles*; McGraw-Hill: New York, 1981.
(63) Darden, T.; York, D.; Pedersen, L. G. *J. Chem. Phys.* **1993**, *98*, 10089–10092.
(64) Essmann, U.; Perera, L.; Berkowitz, M.; Darden, T.; Lee, H.; Pedersen, L. G. *J. Chem. Phys.* **1995**, *103*, 8577.
(65) Cornell, W. D.; Cleplak, P.; Bayly, C. I.; Gould, I. R.; Merz, K. M., Jr.; Ferguson, D. M.; Spellmeyer, D. C.; Fox, T.; Caldwell, J. W.; Kollman, P. A. *J. Am. Chem. Soc.* **1995**, *117*, 5179–5197.
(66) Jorgensen, W. L.; Chandrasekhar, J.; Madura, J. D.; Impey, R. W.; Klein, M. L. *J. Chem. Phys.* **1983**, *79*, 926.
(67) Dunning, T. H. *J. Chem. Phys.* **1989**, *90*, 1007–1023.
(68) Kistler, K. A.; Matsika, S. *J. Phys. Chem. A* **2007**, *111*, 2650–2661.
(69) Schmidt, M. W.; Baldridge, K. K.; Boatz, J. A.; Elbert, S. T.; Gordon, M. S.; Jensen, J. H.; Koseki, S.; Matsunaga, N.; Nguyen, K. A.; Su, S.; Windus, T. L.; Dupuis, M.; Montgomery, J. A. *J. Comput. Chem.* **1993**, *14*, 1347.
(70) Cancès, E.; Mennucci, B.; Tomasi, J. *J. Chem. Phys.* **1997**, *107*, 3032–3041.
(71) Aleman, C. *Chem. Phys.* **1999**, *244*, 151–162.
(72) Aleman, C. *Chem. Phys. Lett.* **1999**, *302*, 461.
(73) Aleman, C. *Chem. Phys.* **2000**, *253*, 13–19.
(74) Lorentzon, J.; Fülscher, M. P.; Roos, B. O. *J. Am. Chem. Soc.* **1995**, *117*, 9265.
(75) Shukla, M. K.; Mishra, P. C. *Chem. Phys.* **1999**, *240*, 319.
(76) Hudock, H. R.; Levine, B. G.; Thompson, A. L.; Satzger, H.; Townsend, D.; Gador, N.; Ullrich, S.; Stolow, A.; Martinez, T. J. *J. Phys. Chem. A* **2007**, *111*, 8500–8508.
(77) Zgierski, M. Z.; Patchkovskii, S.; Fujiwara, T.; Lim, E. C. *J. Phys. Chem. A* **2005**, *109*, 9384–9387.
(78) Fleig, T.; Knecht, S.; Hättig, C. *J. Phys. Chem. A* **2007**, *111*, 5482–5491.
(79) Laikov, D.; Matsika, S. *Chem. Phys. Lett.* **2007**, *448*, 132–137.
(80) Neiss, C.; Saalfrank, P.; Parac, M.; Grimme, S. *J. Phys. Chem. A* **2003**, *107*, 140.
(81) Shukla, M. K.; Leszczynski, J. *J. Comput. Chem.* **2004**, *25*, 768–778.
(82) Schreiber, M.; Silva-Junior, M. R.; Sauer, S. P. A.; Thiel, W. *J. Chem. Phys.* **2008**, *128*, 134110.
(83) Ismail, N.; Blancafort, L.; Olivucci, M.; Kohler, B.; Robb, M. A. *J. Am. Chem. Soc.* **2002**, *124*, 6818.
(84) Merchán, M.; Serrano-Andrés, L. *J. Am. Chem. Soc.* **2003**, *125*, 8108.
(85) Merchán, M.; Serrano-Andrés, L.; Robb, M.; Blancafort, L. *J. Am. Chem. Soc.* **2005**, *127*, 1820.
(86) Sobolewski, A. L.; Domcke, W. *Phys. Chem. Chem. Phys.* **2004**, *6*, 2763.
(87) Zgierski, M. Z.; Patchkovskii, S.; Fujiwara, T.; Lim, E. C. *J. Phys. Chem. A* **2005**, *109*, 8410.
(88) Zgierski, M. Z.; Patchkovskii, S.; Lim, E. C. *J. Chem. Phys.* **2005**, *123*, 1081101.
(89) Blancafort, L.; Robb, M. A. *J. Phys. Chem. A* **2004**, *108*, 10609.
(90) Fulscher, M. P.; Roos, B. O. *J. Am. Chem. Soc.* **1995**, *117*, 2089.
(91) Tomić, K.; Jörg, T.; Marian, C. M. *J. Phys. Chem. A* **2005**, *109*, 8410–8418.
(92) Cisneros, G. A.; Piquemal, J.-P.; Darden, T. A. *J. Phys. Chem. B* **2006**, *110*, 13682.
(93) Cisneros, G. A.; Tholander, S. N.; Parisel, O.; Darden, T. A.; Elking, D.; Perera, L.; Piquemal, J.-P. *Int. J. Quantum Chem.* **2008**, *108*, 1905–1912.
(94) Yoshikawa, A.; Matsika, S. *Chem. Phys.* **2008**, *347*, 393–404.
(95) Karelson, M. K.; Zerner, M. C. *J. Phys. Chem.* **1992**, *96*, 6949–6957.
(96) Kongsted, J.; Mennucci, B. *J. Phys. Chem. A* **2007**, *111*, 9890–9900.
(97) Williams, S. A.; Renn, C. N.; Callis, P. R. *J. Phys. Chem.* **1987**, *91*, 2730–2734.
(98) Voet, D.; Gratzer, W. B.; Cox, R. A.; Coty, P. *Biopolymers* **1963**, *1*, 193.
(99) Du, H.; Fuh, R. A.; Li, J.; Corkan, A.; Lidsey, J. S. *Photochem. Photobiol.* **1998**, *68*, 141.
(100) Clark, L. B.; Peschel, G. G.; Tinoco, I., Jr. *J. Phys. Chem.* **1965**, *69*, 3615.
(101) Abouaf, R.; Pommier, J.; Dunet, H.; Quan, P.; Nam, P.-C.; Hguyen, M. T. *J. Chem. Phys.* **2004**, *121*, 11668–11674.
(102) Tomić, K.; Tatchen, J.; Marian, C. M. *J. Phys. Chem. A* **2005**, *109*, 8410–8418.

JP901601U